



Assessment of Thermal Behavior of a Flat Plate Water Heater Solar Collector at Different Day Times by Computational Fluid Dynamics Method

Farzaneh Sajadipour^a, Kamran Kheiralipour^{a,*}, Esmaeil Mirzaee Ghaleh^b,
Hekmat Rabani^b

^aMechanical Engineering of Biosystems Department, Ilam University, Ilam, Iran

^bMechanical Engineering of Biosystems Department, Razi University, Kermanshah, Iran

Received: 09-11-2021

Accepted: 17-09-2022

Abstract

Water heaters are important tools to use solar energy, as one of the main renewable energy sources, for increasing water temperature. The present research was conducted to predict the outlet fluid temperature of a solar water heater with a flat plate collector by the computational fluid dynamics method. Initially, the ambient temperature, the temperature of the inlet and outlet fluid, and the temperature of the collector were experimentally measured from 10 am to 18 pm every two hours. The fluid flow tubes of the flat plate solar collector were simulated in the ANSYS Fluent Software. The temperature of the outlet fluid was calculated based on the measured variables by the computational fluid dynamics method. For that, the k- ϵ turbulent model was used for simulating the collector in the software. Validation was carried out between experimental data and numerical results. The results of the simulation showed that computational fluid dynamics can predict the outlet fluid temperature with errors between 1 to 22% .In most cases, the predicted temperatures were higher than those of experimented data and higher errors were observed for higher flow rates.

Keywords: Solar energy, Flat plate solar collector, Computational fluid dynamics, Fluid temperature.

DOI: 10.22059/jsr.2022.333698.1227 DOR: 20.1001.1.25883097.2022.7.4.1.6

1. Introduction

Using alternative energy resources is an important strategy to overcome the environmental burdens of finishable fossil fuels [1]. Sunray is an unlimited source of energy that can be considered an ideal solution to solve problems related to energy

and the environment [2]. This fat and high amount of solar energy in the world [3] shows the importance of paying attention to this energy source in meeting the daily needs of human beings [4]. Among all methods for using solar energy, the solar water heater is the easiest and the most economical

*Corresponding Author Email Address: k.kheiralipour@ilam.ac.ir

one. Having enough knowledge about solar radiation, solar energy can be used for water heating in houses and even industry more easily and effectively than other solar energy systems [5]. This method has been favored by many scholars in the past two decades because, in addition to being renewable, home heating costs can be reduced by 70% [6].

The most important part of a solar water heater system is a solar collector that has different types. Solar collectors are a special type of heat exchangers that convert solar energy to heat [5]. The collector is the main part of the solar heating system to transfer the heat to the fluid with minimal heat dissipation. The most widely used type of collector is the flat plate solar collector due to its high performance, ease of construction, and without any moving parts and need for maintenance [7]. The main parts of the solar collector are the absorbing plate, inlet and outlet fluid tubes, air supply system, and chassis [8]. With regard to the benefits and applications of solar water heating systems, their performances must be investigated for optimum adjusting and improving efficiency.

With respect to the field data collection, in addition to the high cost and time spent wishing, there are some limitations in various cases; whereas numerical modeling and simulation are used with low cost and duration time [9-11].

Modeling is always a necessary and important task in the analysis and investigation of real systems. Modeling is a very effective procedure to know the behavior of a system at the same moment or at other times and even simulation of real systems. In engineering, modeling has always been used to design new processes or analysis of existing processes. In this regard, computational fluid dynamics (CFD) includes powerful analytical methods of the systems including heat transfer, fluid flow, and other phenomena. High matching ability, accuracy, and efficiency increased its application in most processes [12]. The CFD method can be applied to model the environment with irregular and complex geometries using integration by part [13].

Yaghoubi and Akbarimoosavi [14] studied heat transfer in the solar parabolic concentrating collector of a solar power plant system. They investigated the

influence of several parameters such as the fluid speed and shape and material of the absorbent tubes. Azimi [15] investigated the effects of the concentrator and reflector on the performance of flat plate solar collector and found that the lens improves the efficiency but the impact of the reflector was more than the concentrator. Basil et al. [16] examined and compared the heat transfer in different solar collectors and concluded that the structure type has a significant impact on heat transfer. The thermal performance and the efficiency of a conventional collector with two types of solar absorbing plates, rectangular, and curved types were compared by Medina Carril et al. [17]. The results of their research showed that the efficiency of the curved type was 25% higher than the rectangular one. Afroza Nahar et al. [18] investigated a hybrid solar system that had both photovoltaic and collector.

Nadi et al. [19] compared the outlet fluid temperature of a solar collector obtained by CFD modeling and artificial neural networks (ANN). The results of their research showed that the CFD data were in agreement with experimental data. Kiran Niak et al. [20] after experimental investigation on U-Tube solar collector system to assess its performance, modeled to predict its performance. Balakin et al. [21] modeled a direct absorption solar collector with magnetic Nano-fluid by CFD. Agathokleous et al. [22] conducted the experimental and modeling study of a solar thermal collector for air heating. Tafarroj et al. [23] modeled a collector containing nano-fluids to predict its performance. Carmona and Palacio [24] conducted research to model a flat plate solar collector with latent heat storage and compared it with experimental data.

The literature reviews showed that solar water heaters can be modeled and simulated by the CFD method, but in the present research, the method was used to simulate a solar water heater under different conditions to evaluate the accuracy of the method at different times of the day. Among different solar collectors, flat plate one has more applications due to its high performance, ease of construction, lack of the presence of moving parts, and no need for maintenance. Due to the importance of the prediction of outlet water, therefore, the goal of the

present research is to predict the outlet temperature of a flat plate solar collector of a water heating system using the CFD method.

2. Materials and Methods

2.1. Solar water heater

The solar water heater made by Solar Polar Co., Isfahan, Iran was considered to be studied. The heater had a forced circulation system consisting of a pump and required devices for the recirculation of water in the tubes. The most important part of a solar water heater is the absorber plate. It included vertical and horizontal pipes. The specifications of the collector have been presented in Table 1 [25].

Table 1. Specifications of the studied flat plate solar collector (Solar Polar Co.).

No.	Parameter	Value
1	Material/Absorber thickness	Aluminum/0.5 mm
2	Number of transparent covers	1
3	Tube material/Thickness	Copper/1mm
4	Tube distance	150 mm
5	Slope	45°
6	The transparent cover pass constant (τ)	0.9
7	Absorption constant (α)	0.81
8	Horizontal tubes	900 mm length, 40 mm diameter
9	Vertical tubes	1600 mm length, 15 mm diameter



Fig. 1. The studied solar heat water [25].

2.2. Thermal sensors

The thermal sensors were placed on the inlet and outlet points to determine the temperature of the environment, absorber plate, and inlet and outlet fluid. The used sensors in the present research were k-type thermocouples with an accuracy of 0.1 °C. The tips of the thermocouples were fixed to the points using aluminum welding.

2.3. Data logger

In order to record the temperature of the different points of the solar water heater an eight-channel data logger device, model: PROVA 800, Taiwan, was used. The data logger has the ability to record the temperature every 1 s but it was used to record the temperature each 2 h from 10:00 to 18:00 o'clock. After recording the temperatures by the data logger, the obtained data was transferred from its memory to a personal computer.

2.4. Data collection

Some experiments were conducted to gather real data in the same sunny condition in May 2018 at Razi University, Kermanshah, Iran. The gathered data were environment, absorber, and inlet and outlet fluid temperature. The data were collected at different times of the day to validate the CFD results at different day times. The experimental conditions and treatments were reported in Table 2.

Table 2. The different conducted tests for modeling flat plate collectors.

Test No.	Time (h)	Flow rate (kg.s ⁻¹)	Temperature (°C)		
			Ambient	Absorber	Inlet fluid
1		0.10	22.5	39.1	31.8
2	10:00	0.14	22.5	39.5	36.0
3		0.20	22.0	39.1	35.5
4		0.10	25.7	50.0	44.6
5	12:00	0.14	25.7	50.1	43.5
6		0.20	25.7	50.0	43.0
7		0.10	28.5	60.1	54.7
8	14:00	0.14	28.6	60.0	54.8
9		0.20	28.5	60.1	54.0
10		0.10	29.6	60.1	56.9
11	16:00	0.14	29.6	61.3	55.3
12		0.20	29.0	61.5	55.0
13		0.10	27.6	49.0	52.3
14	18:00	0.14	25.5	52.9	43.9
15		0.20	25.9	52.6	41.9

After preparing the solar water heater, sensors, and data logger the experiments were done. The ambient temperature, absorber temperature, and inlet and outlet temperature of fluid were determined by the sensors. The experiments were conducted for three days. The data were recorded each 2 h from 10:00 am to 18:00 pm. Also, to evaluate the results of the CFD method, the experiments were done for different fluid flow rates of the collector as 0.1, 0.14, and 0.20 kg.s⁻¹.

2.5. Numerical simulation

For CFD modeling, firstly the goal system must be simulated in software [26-27]. The fluid tubes of the collector were simulated in the environment of ANSYS Fluent 15 software. Due to the symmetry of the tubes, half of them were considered (Fig. 2). To increase the calculation speed organized network with triangular elements was used to mesh the model (Fig. 2). Totally, 112621 nodes and 456265 elements were created for the model after meshing.

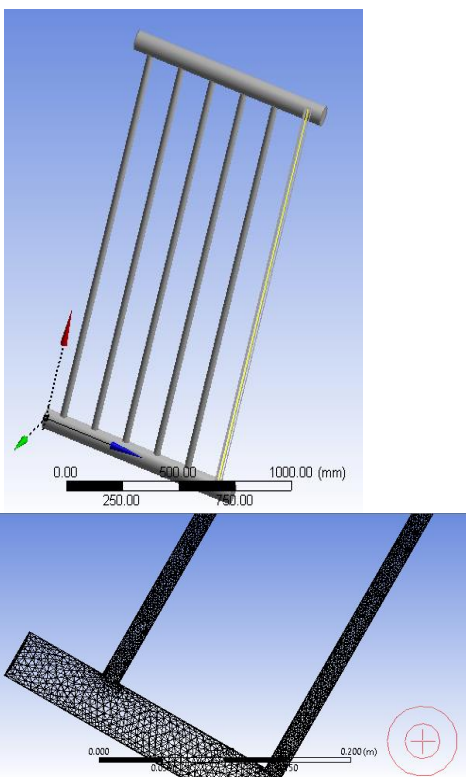


Fig. 2. The simulated tubes of the studied collector (Top) and the meshed model (Bottom) in ANSYS Fluent 15 software.

2.6. Turbulence model

Considering the amount of fluid flow in the present research, 0.1 to 0.2 kg.s⁻¹, the turbulence model was used for numerical calculation of the outlet fluid temperature based on the standard k-ε model [28].

2.7. Boundary conditions

Determination of the boundary conditions is one of the most basic steps in different applications of CFD. It determines the flow and thermal properties in the borders of the considered problem domain according to the problem physics. Boundary conditions in the present research included the temperature of the solar absorber plate, ambient temperature, flow rate, and temperature of inlet fluid. This data was different for each test and so the information related to each test was used for modeling. The used boundary conditions for modeling the flat plate solar collector in the present research were listed in Table 2.

In the present research, after recording the results of the experiments and modeling by CFD, the outlet fluid temperature obtained by both methods was compared to obtain prediction error. The Prediction error was calculated using the following equation.

$$PE = \frac{RM - RE}{RE} \times 100 \quad (1)$$

where PE is the prediction error of CFD modeling, RM is the modeling results, and RE is the experimental results.

3. Results & Discussion

The modeling results by the CFD method, as outlet fluid temperature contours, have been presented in Fig. 4 and Table 3. In Table 3, the outlet fluid temperature calculated by the CFD method and those obtained by experimental tests were compared. The prediction error by the CFD method was calculated by Eq. 3 and listed in Table 3.

As seen in Table 3, the highest error (21.6%) was related to 10:00 o'clock in the morning with a flow rate of 0.10 kg.s⁻¹. The lowest percentage error of 0.1 % was related to 18:00 o'clock with a flow rate of 0.10 kg.s⁻¹. The error between experimental and modeling data may be due to the existence of unknown or uncontrolled environmental factors such as wind. The negative errors in Table 3 showed that the calculated outlet fluid temperature by the CFD

has been less than those obtained in the experimental tests also these cases were observed from 16:00 to 18:00 o'clock.

Table 3. Comparison of the results obtained by CFD modeling and experiments.

Test No.	Time (h)	Flow rate (kg.s ⁻¹)	Outlet fluid temperature (°C)		Error (%)
			Experimental	Modeling	
1	10:00	0.10	33.6	40.9	21.6
2		0.14	37.0	38.9	5.0
3		0.20	36.5	37.9	3.7
4	12:00	0.10	46.7	52.9	13.2
5		0.14	47.2	48.9	3.5
6		0.20	46.9	47.9	2.0
7	14:00	0.10	56.0	56.9	1.5
8		0.14	56.1	58.9	4.9
9		0.20	56.4	58.9	4.3
10	16:00	0.10	57.4	56.9	-0.1
11		0.14	57.3	60.9	6.2
12		0.20	56.3	57.9	-2.8
13	18:00	0.10	53.2	51.9	-2.5
14		0.14	49.9	49.9	-0.1
15		0.20	48.3	47.9	-0.9

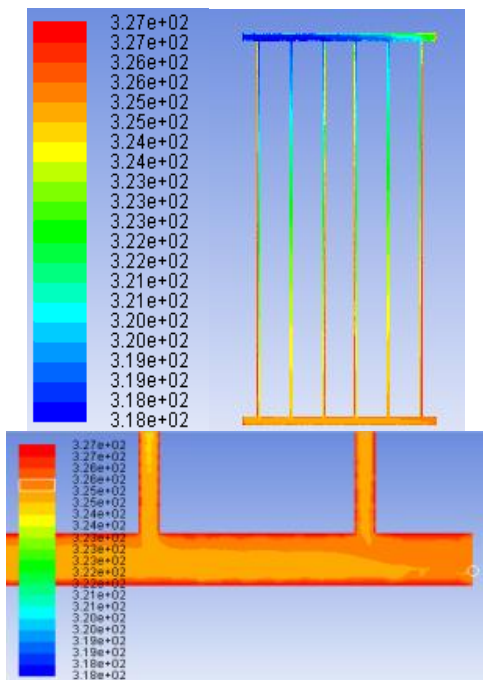


Fig. 3. The outlet fluid temperature counter for the flow rate of 0.10 kg.s⁻¹ at 12:00 o'clock.

3.1. Comparing the experimental and modeling results

After solving the problem by the CFD method and ANSYS Fluent Software, the obtained results for all models have been recorded (Fig. 4).

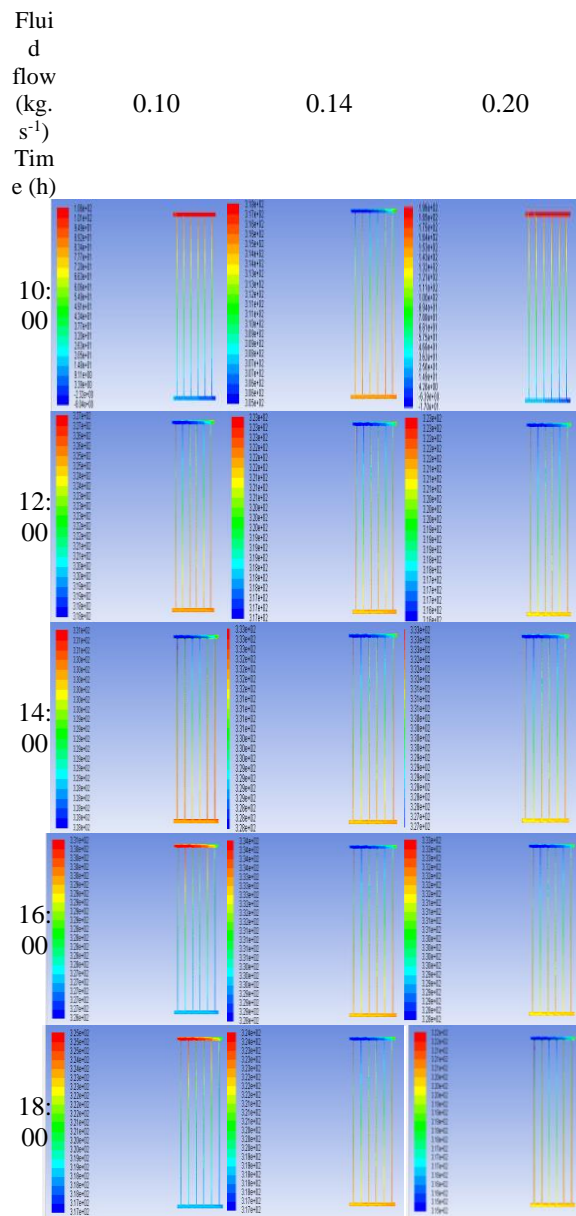


Fig. 4. The contour results of all CFD models.

3.2. Temperature variation at different times

The differences between real outlet fluid temperatures obtained by experiments and modeled CFD results at different day times from 10:00 am to

18:00 pm for each 2 h and all studied flow rates have been presented in Fig. 5-7.

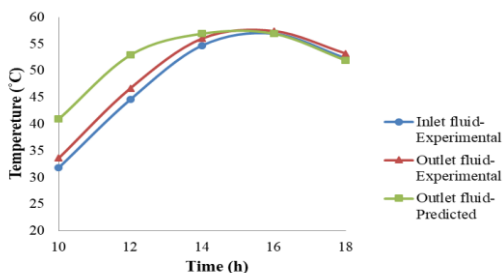


Fig. 5. The differences between outlet fluid temperatures obtained by experiments and CFD modeling at different times and 0.10 kg.s⁻¹ flow rates.

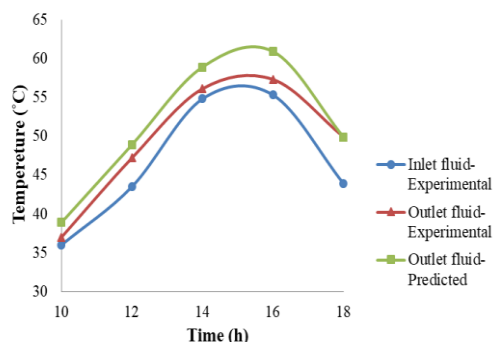


Fig. 6. The differences between outlet fluid temperatures obtained by experiments and CFD modeling at different times and 0.14 kg.s⁻¹ flow rates.

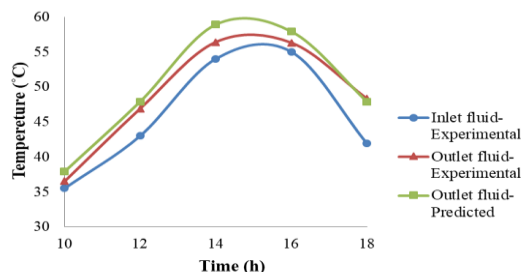


Fig. 7. The differences between outlet fluid temperatures obtained by experiments and CFD modeling at different times and 0.20 kg.s⁻¹ flow rates.

For 0.10 kg.s⁻¹ flow rates in Fig. 5, the modeling errors were high from 10:00 to 12:00 am, whereas those were very low from 14:00 to 18:00 pm. The modeling errors for 0.14 and 0.20 kg.s⁻¹ in Fig. 6-7

were the same. The errors were high from 14:00 to 16:00 pm and those were low for other day times.

3.3. Flow rate

The differences between outlet fluid temperatures obtained by experimental tests and CFD modeling at different flow rates for all studied day times have been presented in Fig. 8-12.

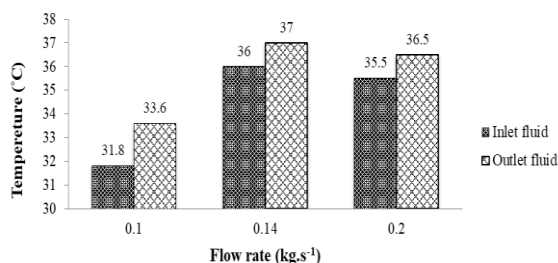


Fig. 8. The differences between outlet fluid temperature obtained by experiments and CFD modeling at different flow rates and 10:00 o'clock.

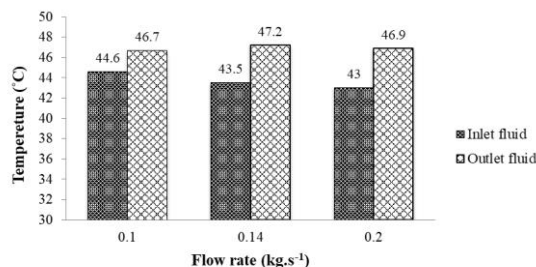


Fig. 9. The differences between outlet fluid temperature obtained by experiments and CFD modeling at different flow rates and 12:00 o'clock.

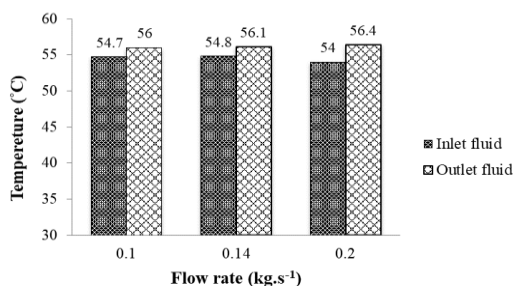


Fig. 10. The differences between outlet fluid temperature obtained by experiments and CFD modeling at different flow rates and 14:00 o'clock.

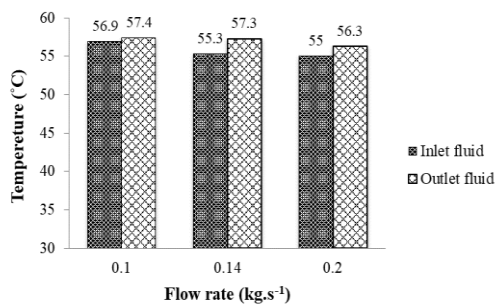


Fig. 11. The differences between outlet fluid temperature obtained by experiments and CFD modeling at different flow rates and 16:00 o'clock.

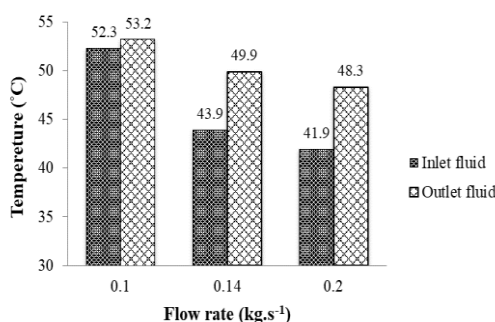


Fig. 12. The differences between outlet fluid temperature obtained by experiments and CFD modeling at different flow rates and 18:00 o'clock.

At 10:00 am the difference between real and predicted outlet temperatures for 0.14 and 0.20 kg.s⁻¹ flow rates was the same and equal to 1 °C but it had a higher value for 0.10 kg.s⁻¹ as 1.8 °C. The temperature differences for 0.10 kg.s⁻¹ (2.1 °C) were lower than those for other flow rates at 12:00 o'clock (> 3 °C). At 14:00 o'clock, the difference for 0.20 kg.s⁻¹ was higher (2.4 °C) than those of other flow rates (1.3 °C). The difference between the real and predicted temperature at 16:00 o'clock was ranked as 0.14, 0.20, and 0.10 kg.s⁻¹ with values of 2, 1.3, and 0.5 °C, respectively. Highest temperature differences were observed in Fig. 12 at 18:00 o'clock for 0.14 (6 °C) and 0.20 kg.s⁻¹ (6.4 °C). Also in this condition, the difference for 0.10 kg.s⁻¹ was lower (0.9 °C).

According to Fig. 8-12, totally can be told that the heat transfer between absorber and fluid is better in lower flow rates and thus there is expected that the temperature difference between inlet and outlet fluid to be increased. The reason for this difference is the lower speed of the fluid passing from the

collector tubes and so the fluid had more opportunities to have better heat exchange. But in higher flow rates the fluid has a lower time for heat exchange with the absorber plate resulting in a higher temperature difference between real and modeled results and so lower CFD modeling accuracy.

4. Conclusions

In the present research, as time passed from the morning, the outlet fluid temperature increased gradually due to the amount of solar radiation that increases resulting in an increase of absorbed energy and so it was maximum at noon. With reduce in flow rate, the amount of the transferred energy from the collector to the fluid increases, and thus the temperature of the outlet fluid increases. The differences between the temperature of the inlet and outlet fluids in the range of 10:00 am to 18:00 pm initially increased and then it had a descending trend. The temperature of the outlet fluid at a flow rate of 0.10 kg.s⁻¹ was the highest and 0.20 kg.s⁻¹ had the lowest value. At the beginning of the day, with an increase in inlet temperature, the outlet fluid temperature increased while as time passed the outlet fluid temperature decreased.

The maximum temperature difference between experimental real data and the predicted numerical results calculated by the CFD method was about 7.3 °C related to a 0.10 kg.s⁻¹ flow rate at 10:00 o'clock and the corresponding percentage error was obtained as 21.6%. The predicted outlet fluid temperature at 10-14 o'clock was more than those obtained by experiments whereas at 16-18 the opposite results were obtained. For different tests, the temperature of the outlet fluid by experiments and CFD modeling had in agreed and its predicting error was between 0.1 to 21.6%.

Acknowledgments

The authors thank Ilam University and Razi University for their support in the research.

References

- [1] Khoobbakht, G., Kheiralipour, K., Karimi, M. (2022). The effects of biodiesel and bioethanol on the performance and emission characteristics of diesel engines. *International Journal of Renewable Energy Resources*, 12(1), 1-23.

- [2] Mahboub, R., Kheiralipour, K. (2022). The effect of dust storm on the performance of photovoltaic panel at different tilt angles. *Journal of Energy Engineering & Management*, 12(2), 72-81.
- [3]. Breeze, P. (2019). *Power Generation Technologies*. 3rd Ed. Elsevier, the Netherlands.
- [4] Mahboub, R., Kheiralipour, K. (2022). Development of the performance loss models for a photovoltaic panel under the influence of dust deposition. *Energy Systems*, <https://doi.org/10.1007/s12667-022-00520-9>.
- [5] Zanjani, M. (2011). Predicting the optimal flow rate of a flat plate solar collector by artificial intelligence. M.Sc. Thesis. Razi University. 2011. (In Persian).
- [6] Selmi, M., Al-Khawaja, M.J. and Marafia, A. (2008). Validation of CFD simulation for flat plate solar energy collector. *Renewable Energy*, 33, 383-373.
- [7] Khorami Fard, M. (2013). Experimental investigation and numerical analysis of physical and environmental parameters of flat plate solar collector on its performance. M. Sc. Thesis. Isfahan University of Technology, Iran. (In Persian).
- [8] Mahdavi Adeli, M., Dastanian, M. and Farahat, S. (2013). Design, construction and evaluation of a solar thermal photovoltaic system with Nano-fluid coolant. 3rd International Conference on new approaches in energy preservation, Tehran, Iran. (In Persian).
- [9] Rasekh, M., Asadi, M.R., Jafari, A. and Kheiralipour, K. (2009). Obtaining Maximum Stresses in Different Parts of Tractor (Mf-285) Connecting Rods Using Finite Element Method. *Australian Journal of Basic and Applied Sciences*, 3(2), 1438-1449.
- [10] Jahanbakhshi, A., Heidari Raz Dareh, S. and Kheiralipour, K. (2017). Stress Analysis of Crossbar of Moldboard Plough Pulled by Massey Ferguson 285 and 299 Tractors. *Advances in Applied Sciences*, 2(1), 11-17.
- [11] Asadi, M.R., Rasekh, M., Golmohammadi, A., Jafari, A., Kheiralipour, K. and Borghei, A.M. (2010). Optimization of connecting rod of MF-285 tractor. *Journal of Agricultural Technology*, 6(4), 649-662.
- [12] Norton, T. and Sun, D.W. (2006). Computational fluid dynamics (CFD)-An effective and efficient design and analysis tool for the food industry: A Review. *Trends in Food Science and Technology*, 17, 600-620.
- [13] Boustani, A. (2009). Modeling of the platform and pipe in urban water distribution network by finite element method. M.Sc. Thesis. Sari University, Iran. (In Persian).
- [14] Yaghoubi, M. and Akbarimoosavi, M. (2011). Three dimensional thermal expansion analysis of an absorber tube in a parabolic trough collector. *Solar PACES*, Granada, Spain.
- [15] Azimi, A. (2011). Analytical and experimental study the effects of the use of the concentrator and flat reflector on the performance of a flat plate solar collector. M.Sc. Thesis. Kashan University, Iran. (In Persian).
- [16] Basil, H., Ali, S., Gilani, I. and Al-Kayiem, H. (2014). A three dimensional performance analysis of a developed evacuated tube collector using a CFD fluent solar load model. *MATEC Web of Conference*, 13, 06011.
- [17] Medina Carril, D.M., Carrillo, J.G., Maldonado, R.D. and Aviles, F. (2016). Finite element analysis of a solar collector plate using two plate geometries. *Ingeniería e Investigación*, 36, 95-101.
- [18] Afroza Nahar, M., Hasanuzzaman, N. and Rahim, A. (2017). Numerical and experimental investigation on the performance of a photovoltaic thermal collector with parallel plate flow channel under different operating conditions in Malaysia. *Solar Energy*, 144, 517-528.
- [19] Nadi, F., Abdanan Mehdizadeh, S. and Nourani Zonouz, A. (2016). Comparing between predicted output temperature of flat-plate solar collector and experimental results: computational fluid dynamics and artificial neural network. *Journal of Agricultural Machinery*, 7, 298-311. (In Persian).
- [20] Kiran Niak, B., Bhowmik M. and Muthukumar, P. (2019). Experimental investigation and numerical modelling on the performance assessments of evacuated U-Tube solar collector systems. *Renewable Energy*, 134, 1344-1361.
- [21] Balakin, B.V., Zhdaneev, O.V., Kosinska, A. and Kutsenko, K.V. (2019). Direct absorption solar collector with magnetic nanofluid: CFD model and parametric analysis. *Renewable Energy*, 136, 23-32.
- [22] Agathokleous, R., Barone, G., Buonomano, A., Forzano, C., Kalogirou, S.A. and Palombo, A. (2019). Building façade integrated solar thermal collectors for air heating: experimentation, modelling and applications. *Applied Energy*, 239, 658-679.

- [23] Tafarroj, M. M., Daneshazarian, R. and Kasaeian, A. (2019). CFD modeling and predicting the performance of direct absorption of nanofluids in trough collector. *Applied Thermal Engineering*, 148, 256-269.
- [24] Carmona, M. and Mario Palacio, M. (2019). Thermal modelling of a flat plate solar collector with latent heat storage validated with experimental data in outdoor conditions. *Solar Energy*, 177, 620-633.
- [25] Dehlaghi, L., Rabbani, H., Mirzaee Ghaleh, E. and Kheiralipour, K. (2019). Forecasting the outlet fluid temperature from a flat plate collector using artificial neural networks (ANNs) and support vector regression (SVR). *Iranian Journal of Biosystems Engineering*, 49(4), 669-678. (In Persian).
- [26] Jahanbakhshi, A., Heidari Raz Dareh, S. and Kheiralipour, K. (2020). Finite element fatigue analysis of mouldboard plough cross bar based on the draft force of MF 399 Tractor. *Journal of Failure Analysis and Prevention*, 20, 2106–2110.
- [27] Yousefi, S., Farsi, H. and Kheiralipour, K. (2016). Drop test of pear fruit: experimental measurement and finite element modelling. *Biosystems Engineering*, 147, 17-25.
- [28] Tohidi, A. (2013). *ANSYS Fluent Guide*. Dibagaran Artifice Kultur Institute. Tehran. (In Persian).